Information-transferring ability of the different phases of a finite *XXZ* spin chain

Abolfazl Bayat and Sougato Bose

Department of Physics and Astronomy, University College London, Gower Street, London WC1E 6BT, United Kingdom

(Received 17 December 2008; revised manuscript received 19 October 2009; published 6 January 2010)

We study the transmission of both classical and quantum information through all the phases of a finite *XXZ* spin chain. This characterizes the merit of the different phases in terms of their ability to act as a quantum wire. As far as quantum information is concerned, we need only consider the transmission of entanglement as the direct transmission of a quantum state is equivalent. The isotropic AFM spin chain is found to be the optimal point of the phase diagram for the transmission of quantum entanglement when one considers both the amount of transmitted entanglement and the velocity with which it is transmitted. However, this optimal point in the phase diagram moves to the Néel phase when decoherence or thermal fluctuations are taken to account. This chain may also be able to transfer classical information even when, due to a large magnitude of the noise, quantum information is not transmitted at all. For a certain range of anisotropies of the model, a curious feature is found in the flow of quantum information inside the chain, namely, a hopping mode of entanglement transfer which skips the odd-numbered sites. Our predictions will potentially be testable in several physical systems.

DOI: 10.1103/PhysRevA.81.012304 PACS number(s): 03.67.Hk, 75.10.Pq, 03.65.Ud

I. INTRODUCTION

Recently, condensed-matter many-body systems have been viewed in the light of quantum information. For example, the entanglement inherent in these systems has been investigated [1]. One can, however, ask a different question: How does information placed on one part of a many-body system *pass through* such a system? Aside from its fundamental interest, this question may lead to mechanisms for moving information over small distances. The idea is to use a finite many-body system such as a spin chain (a chain of perpetually interacting stationary spins—a one-dimensional magnet) as a data bus [2]. Many-body dynamics transports information placed on a spin at one end of the chain to the spin at its other end with a certain efficiency. This is an "all solid-state" bus whose spins and interactions, except for those at its very ends, are never controlled. Applications could be in moving information between quantum registers or for moving classical bits in nanoscale spintronics. This idea has several benefits for practical applications: (i) since quantum registers are expected to be solid-state systems, using a solid-state wire for their communication avoids the complexity of converting the information from one carrier to another; (ii) any external control on a quantum system demands some macroscopic devices which potentially destruct the fragile entanglement coherence, so minimal control on just two ends of an spin chain minimizes the decoherence. This area, reviewed in [3], has mainly focused on perfecting the information transfer (information transmission) by clever means: special couplings [4], encoding [5], pulsing [6], etc. The inevitable destructive effects of, for example, thermal fluctuations [7] and decoherence [8] also have been taken to account. The memory effect in these kinds of quantum channels has been studied to decrease the hardware complexity and increase the rate [9]. However, most of the former spin-chain quantum communication studies are focused on ferromagnetic systems; the AFM systems have been introduced as even better and faster alternatives [10].

An interesting question from a condensed-matter angle is how the above process of information transmission varies with the phase of the spin chain. By "phase" we mean both the form of the spin-spin interactions and the relevant ground state resulting from that interaction. In this context, only one study has been performed, which involves spin-1 chains [11]. Additionally, gapless phases have been shown to be generically bad for a "slow" information transmission process that can take place between two spins coupled weakly to a many-body system [12]. The same slow information transmission process between spins coupled weakly to an anti-ferromagnetic (AFM) chain has also been studied [13]. However, there has been no investigation yet of information transmission as a function of the phases of the simplest case, namely the spin-1/2 chain, when all spins are coupled with equal strength, so that information transmission is fast. Instead, a majority of the work has simply assumed a fully polarized (symmetry broken) ferromagnetic (FM) initial state of the spin chain [3]. Here we study the process of information transfer through all phases of an $S = 1/2$ *XXZ* Heisenberg-Ising chain, which models a range of realistic materials and, according to Ref. [14], is the most important paradigm in low-dimensional quantum magnetism. Using finite chains (the case relevant for information transmission) and exact diagonalization, we identify the point in the phase diagram which provides the optimal data bus in absence of any encoding, engineering, control, etc. Interestingly, this turns out to be the "isotropic" AFM phase, which is the most interesting phase [14] of the *XXZ* model. Here the ground state has complete SU(2) symmetry and contains significant "quantum" correlations or entanglement. This phase is, perhaps, also the most common, as it appears in the ubiquitous Hubbard model at strong repulsion and half filling. Additionally, most solid-state spin chains such as the famous $KCuF_3$ [14], engineered atomic-scale spin chains [15], and doped fullerine $Sc@C_{82}$ chains [16] are naturally AFM.

This study is an example of nonequilibrium dynamics in many-body systems, currently a topic of intense activity [17]. Our dynamics is induced by suddenly coupling a single spin (the one bearing the information) with one end of a finite spin chain. For a range of phases, certain spin correlation functions behave curiously in this dynamics so that the initial state of the added spin *hops* through the chain *skipping alternate sites*. Additionally, information transmission exhibits contrasting

behavior in the FM and AFM parts of the so-called *XY* phase and has a sharp jump at the boundary of the *XY* and FM phases.

The structure of this article is as follows: In Sec. II we show that entanglement distribution through an arbitrary channel is equivalent to the process of transferring a quantum state through the channel. In Sec. III we introduce our model, that is, an *XXZ* Hamiltonian, and in Sec. IV we consider the entanglement distribution via whole phase diagram of an *XXZ* chain. This is followed by an explanation in Sec. V. In Sec. VI we characterize the effect of the channel. In Secs. VII and VIII, the thermal fluctuations and interactions with a bath, respectively, are investigated. Classical communication through this system is the subject of Sec. IX, which is followed by considering the information flow "inside the chain" in Sec. X. In Sec. XI, we give some potential physical realizations which might test our results, while we summarize our results in Sec. XII.

II. EQUIVALENCE OF STATE TRANSFERRING AND TELEPORTATION MODELS OF INFORMATION TRANSMISSION

In order to transfer information from one place to another, we have to transfer a state (say the state of a spin) which encodes some information. In particular, when we are thinking about quantum information transmission, to quantify the quality of transmission, we compute the fidelity between the sent and the received state. Since this fidelity is dependent on the initial state, it is preferable to take the average value of the fidelity over all possible equiprobable initial states. This average fidelity makes it possible to compare transmission quality of different channels and different schemes of information transmission. To send quantum information from sender to receiver, one can think about two different strategies. In the first strategy, which is called "quantum state transferring," the quantum state is sent through the channel directly. Because of the interaction between the channel and the quantum state, they become entangled and state transferring is imperfect in the sense that the fidelity between the received state and the initial state is less than one. On the other hand, instead of using state transferring, one can use teleportation for sending quantum information. Teleportation is based on a shared entangled pair between sender and receiver which plays the role of the resource [18]. In this second strategy of sending quantum information, the sender generates a maximally entangled pair, keeps one part, and sends the other one to the receiver through the channel. This shares an entangled pair between both sides of the channel and teleportation between sender and receiver can be used for information transmission. However, this fact that the entanglement of the shared pair is not maximal makes the teleportation imperfect. The importance of the second strategy is that we send just one part of the singlet state through the channel and it is not necessary to study the effect of the channel on an arbitrary state. What we show in this section is that the average fidelity in both strategies are the same. This was already shown in [19] using a different technique for arbitrary dimensions of the Hilbert spaces and here we prove it again, just for qubits, using a much simpler language.

Let's start with the state transferring. In this case, quantum state goes through the channel. An arbitrary quantum channel ξ is completely determined by a set of Kraus operators $\{K_m\}$ such that the output of the channel is

$$\rho_r^{\mathrm{ST}} = \xi(\rho_s) = \sum_m K_m \rho_s K_m^\dagger, \quad \sum_m K_m^\dagger K_m = I, \tag{1}$$

where ρ_s is the input state of the channel, ρ_r is the output state received by the receiver, and ST stands for "state transferring." Here we start from the most general form of a qubit state $|\psi_s\rangle = \cos\theta/2|0\rangle + e^{i\phi}\sin\theta/2|1\rangle$ as the input. After interacting the pure input state $\rho_s = |\psi_s\rangle\langle\psi_s|$ with the channel, the output state ρ_r^{ST} [given by Eq. (1)] is generally a mixed state. Fidelity between the received and the sent states is easily computed as $F^{\mathrm{ST}}(\theta,\phi) = \langle\psi_s|\rho_r^{\mathrm{ST}}|\psi_s\rangle$, which is dependent on input parameters θ and ϕ. To get an input independent quantity, we average the fidelity over all possible input states, that is, the surface of the Bloch sphere, with uniform weight. With a straightforward computation we end up with

$$F_{\mathrm{av}}^{\mathrm{ST}} = \frac{1}{4\pi}\int F^{\mathrm{ST}}(\theta,\phi)\sin\theta d\theta d\phi = \frac{1}{3} + \frac{1}{6}\sum_m |\mathrm{Tr}(K_m)|^2, \tag{2}$$

where $\mathrm{Tr}(\cdot) = \mathrm{Trace}(\cdot)$.

Now, we try to use the teleportation strategy for sending quantum information. To achieve this strategy we prepare a pair of singlet state,

$$|\psi^-\rangle = \frac{|01\rangle - |10\rangle}{\sqrt{2}}. \tag{3}$$

Then we keep one part of the pair in the sender and send the other part through the channel ξ. Since the first part in the sender does not interact with the channel, the whole effect of the channel is explained by

$$\rho_{\mathrm{out}} = I\otimes\xi(|\psi^-\rangle\langle\psi^-|) = \sum_m I\otimes K_m|\psi^-\rangle\langle\psi^-|I\otimes K_m^\dagger. \tag{4}$$

Generally, the output state ρ_{out} is not a maximally entangled state, so when it is used as the resource of the standard teleportation scheme [18], it gives an imperfect teleportation in the sense that the final achievable fidelity is less than one. In [20] it has been shown that teleporting ρ_s using noisy resource ρ_{out} generates the following state as the output of the teleportation:

$$\rho_r^{\mathrm{TP}} = \sum_{m=0}^{3}\mathrm{Tr}(\rho_{\mathrm{out}}E_m)\sigma_m\rho_s\sigma_m, \tag{5}$$

where TP stands for "teleportation," $E_m = \sigma_m|\psi-\rangle\langle\psi - |\sigma_m$, and σ_m are Pauli matrices ($\sigma_0 = I$, $\sigma_{1,2,3} = \sigma_{x,y,z}$). Similar to the first strategy, fidelity of the received and the sent states is defined as $F^{\mathrm{TP}}(\theta,\phi) = \langle\psi_s|\rho_r^{\mathrm{TP}}|\psi_s\rangle$ and average fidelity for input states is easily computed over the surface of the Bloch sphere. The average fidelity of the teleportation scheme is

$$\begin{aligned} F_{\mathrm{av}}^{\mathrm{TP}} &= \frac{1}{4\pi}\int F^{\mathrm{TP}}(\theta,\phi)\sin(\theta)d\theta d\phi \\ &= \mathrm{Tr}(E_0\rho_{\mathrm{out}}) + \frac{1}{3}\sum_{m=1}^{3}\mathrm{Tr}(E_m\rho_{\mathrm{out}}) \\ &= \frac{1+2\mathrm{Tr}(E_0\rho_{\mathrm{out}})}{3}. \end{aligned} \tag{6}$$

The parameter $\mathrm{Tr}(E_0\rho_{\mathrm{out}}) = \langle\psi^-|\rho_{\mathrm{out}}|\psi^-\rangle$ is called a *singlet fraction* and as it is clear from Eq. (6) that it completely captures the quality of the transmission. It is also clear from Eq. (6) that to have an average fidelity above 2/3, which is accessible to the classical teleportation, a singlet fraction should exceed 1/2. Using the form of ρ_{out} in Eq. (4) and expanding the singlet as in Eq. (3), one gets $\mathrm{Tr}(E_0\rho_{\mathrm{out}}) = \frac{1}{4}\sum_m |\mathrm{Tr}(K_m)|^2$. Substituting this value in Eq. (6) shows that $F_{\mathrm{av}}^{\mathrm{TP}} = F_{\mathrm{av}}^{\mathrm{ST}}$.

Getting identical average fidelity in both strategies is a very important result in quantum communication, which shows the average effect of a channel can be captured just by transferring one part of the singlet state through the channel and computing the singlet fraction. However, sharing an entangled pair between sender and the receiver has an advantage, namely that after a few transmissions the total (generally noisy) entanglement can be converted by local actions [21] to nearly a pure singlet. This can be used to transmit any state near perfectly using quantum teleportation. So, because of the importance of the amount of entanglement shared between the sender and the receiver and its proven equivalence to the more straightforward transmission of quantum states, we mainly focus on the entanglement distribution through the phase diagram of the *XXZ* Hamiltonian.

III. INTRODUCING THE MODEL

We consider a spin chain as a channel for information transferring and we study the property of each phase of the chain on the quality of information transmission. We take one of the most well-known models in condensed-matter physics, namely a *XXZ* spin chain. The Hamiltonian of the open *XXZ* chain of length N_{ch} is

$$H_{\mathrm{ch}} = J\sum_{i=1}^{N_{\mathrm{ch}}-1}\left\{\sigma_i^x\sigma_{i+1}^x + \sigma_i^y\sigma_{i+1}^y + \Delta\sigma_i^z\sigma_{i+1}^z\right\}, \qquad (7)$$

with J being a coupling constant, Δ being the anisotropy, and $\sigma_k^{x,y,z}$ being Pauli matrices for site k. This Hamiltonian has a rich phase diagram. For $\Delta = 1$ and $J < 0$, this interaction is the FM Heisenberg chain widely discussed in the context of quantum communication [2–4]. More interesting regimes exist for $J > 0$ and different values of Δ [14]. $\Delta < -1$ is the FM phase with a simple separable biased ground state with all spins aligned to the same direction. $-1 < \Delta \leqslant 1$ is called XY phase, which is a gapless phase and consists of two different legs, the FM half ($-1 < \Delta < 0$) and the AFM part ($0 \leqslant \Delta \leqslant 1$). $1 < \Delta$ is called *Néel phase*, where the spectrum is gapped and we get nonzero staggered magnetization. In the limit $\Delta \gg 1$ it takes the form of Néel states ($|010101\ldots01\rangle$).

IV. INFORMATION TRANSMISSION THROUGH A WHOLE-PHASE DIAGRAM OF THE *XXZ* HAMILTONIAN

Though information transmission can be investigated either classically or quantum mechanically, we will primarily examine quantum information transmission and devote one section later to classical information transmission in the same systems. Of course, the most natural setting would be sending the state of a single spin through the chain. However, because of previous "equivalency" discussions in Sec. II, we will examine the transmission of one part of a two-spin maximally entangled state of the form (3) while a spin-chain channel (spins 1 to N_{ch}) is in its ground state of some Hamiltonian H_{ch}. At time $t = 0$, the interaction of the 0th and the 1st spin is suddenly switched on while $0'$ is kept isolated from the rest. The ensuing dynamics transports the initial state of the 0th spin through the chain to the N_{ch}th spin with some efficiency, so that after a while $0'$ will be entangled with N_{ch}. As the singlet has the same representation in any basis, the above entanglement transfer already subsumes within it "state transfer in arbitrary basis" and is thus very general.

The reader may naturally question how general the above physical setting (couplings, etc.) of transferring entanglement through a spin-chain channel is. Indeed, one could have taken weaker or stronger or different couplings at the sending and receiving ends. However, weaker couplings generally lead to "slow" transfer schemes which will be susceptible to decoherence. On the other hand, if we really do have stronger couplings or different couplings available at our disposal, we could just use them for the whole chain for faster and potentially better transfer, rather than using those special couplings only at the ends. So we think that the most natural way to investigate this question is to simply place a spin encoding the unknown state to be transmitted at one end of the chain and couple it with the same coupling as present in the rest of the chain (which, as we know from the previous section, is equivalent to the type of entanglement transmission considered by us). In any case, without putting some restrictions on the coupling model at the ends, there is too much freedom in the problem, and it may not be possible to give a precise answer to the effectiveness of a phase to transfer quantum information. Moreover, also note that we are not considering the generation of entanglement from inside the spin chain, which is an altogether different problem [22], but merely the *transmission* of entanglement through the chain.

Note that for our scheme we require the chain initially in a unique ground state $|\psi_g\rangle_{\mathrm{ch}}$ and this may have to be selected out by applying an arbitrarily small magnetic field (for odd N_{ch} AFM chain and the FM chain). The interaction between the 0th and the 1st spins (the interaction turned on at $t = 0$) of the channel is assumed to be of the same form and strength as the rest of the interactions, namely,

$$H_I = J\left(\sigma_0^x\sigma_1^x + \sigma_0^y\sigma_1^y + \Delta\sigma_0^z\sigma_1^z\right). \qquad (8)$$

With the $0'0$ singlet, the total length of the system considered is thus $N = N_{\mathrm{ch}} + 2$, with the initial state being

$$|\psi(0)\rangle = |\psi^-\rangle_{0'0} \otimes |\psi_g\rangle_{\mathrm{ch}} \qquad (9)$$

and the total Hamiltonian being

$$H = I_{0'} \otimes (H_{\mathrm{ch}} + H_I), \qquad (10)$$

so that $0'$ never interacts with the rest. Also note that H is simply a Hamiltonian of a single spin chain $0\ldots N_{\mathrm{ch}}$ of length $N + 1$. As the aim is entanglement distribution, we are interested at the times at which the entanglement between spins $0'$ and N_{ch} peaks. By turning on the interaction between spin 0 and spin 1 of the channel, the initial state evolves to the state $|\psi(t)\rangle = e^{-iHt}|\psi(0)\rangle$ and one can compute the density matrix

$\rho_{ij} = \mathrm{tr}_{\hat{ij}}\{|\psi(t)\rangle\langle\psi(t)|\}$, where the meaning of $\mathrm{tr}_{\hat{ij}}$ is the trace over whole of the system *except* sites i and j. (We fix $i = 0'$ in this article.) The general form of a two spin density matrix ρ_{ij} in XXZ systems in the computational $(|00\rangle, |01\rangle, |10\rangle, |11\rangle)$ basis is [23]

$$\rho_{ij} = \begin{pmatrix} u^+ & 0 & 0 & 0 \\ 0 & w^+ & z & 0 \\ 0 & z & w^- & 0 \\ 0 & 0 & 0 & u^- \end{pmatrix}, \tag{11}$$

where all the elements of the matrix are real and they can be written in terms of one- and two-point correlations,

$$\begin{aligned} u^{\pm} &= \tfrac{1}{4}\{1 + \langle\sigma_i^z(t)\sigma_j^z(t)\rangle \pm \langle\sigma_i^z(t)\rangle \pm \langle\sigma_j^z(t)\rangle\}, \\ w^{\pm} &= \tfrac{1}{4}\{1 - \langle\sigma_i^z(t)\sigma_j^z(t)\rangle \mp \langle\sigma_i^z(t)\rangle \pm \langle\sigma_j^z(t)\rangle\}, \\ z &= \tfrac{1}{4}\{\langle\sigma_i^x(t)\sigma_j^x(t)\rangle + \langle\sigma_i^y(t)\sigma_j^y(t)\rangle\}, \end{aligned} \tag{12}$$

where $\sigma_j^{\alpha}(t) = e^{iHt}\sigma_j^{\alpha}e^{-iHt}$ (for all $\alpha = x, y, z$) is the Heisenberg picture of σ_j^{α} and $\langle\rangle$ means expectation value according to the initial state (9). The concurrence as a measure of entanglement [24] for this general density matrix (11) is $E = 2\max(0, |z| - \sqrt{u^+u^-})$, which is a function of time-dependent correlators and expectation values. Noteworthy is that for $\Delta > -1$, when the initial state of the channel is *not* symmetry broken, symmetry considerations and the fact that 0 and $0'$ are initially anti-correlated in a singlet imply that the entanglement between $0'$ and j can be written as

$$E_{0'j} = \max\left[0, \left|\langle\sigma_0^x(0)\sigma_j^x(t)\rangle\right| - \tfrac{1}{2}\langle\sigma_0^z(0)\sigma_j^z(t)\rangle - \tfrac{1}{2}\right], \tag{13}$$

which is solely written in terms of the two-time correlation functions of the spin chain $0 \ldots N_{\mathrm{ch}}$. It should be noticed that though two-point correlations of the XXZ Hamiltonian have been studied intensively in the literature and their asymptotic behavior is known, the correlations here are different since they are computed in terms of the initial state (9), which is not the ground state of H. In addition, if one ignores (traces out) spin $0'$, our study can be regarded as an analysis of two-time correlation functions during the nonequilibrium dynamics that ensues when the interaction of a spin in a random state with one end of a spin chain is switched on. Singlet fraction of the state $\rho_{0'N}$, which was shown to be directly related to the average fidelity of state transferring, can be computed also from $\rho_{0'N}$ easily:

$$F = \langle\psi^-|\rho_{0'N}|\psi^-\rangle = \tfrac{1}{2}(w^+ + w^- - 2z). \tag{14}$$

In Fig. 1 we plot both entanglement and singlet fraction of $\rho_{0'N}$ in terms of time for a particular point in the phase diagram, namely $\Delta = 1$. As can be seen from figure, singlet fraction always oscillates while the entanglement just peaks at certain times, which we call optimal time t_{opt}. When entanglement peaks, singlet fraction also has a peak, which shows that final state is more similar to singlet than other Bell states. The time that one can afford to wait for the entanglement between $0'$ and N_{ch} to attain a peak is restricted by practical considerations, such as the decoherence time, required speed of connections in a quantum network, etc. So we restrict ourselves to the first peak of the entanglement in time. To compare the performance of different phases of the Hamiltonian (7) in transferring the

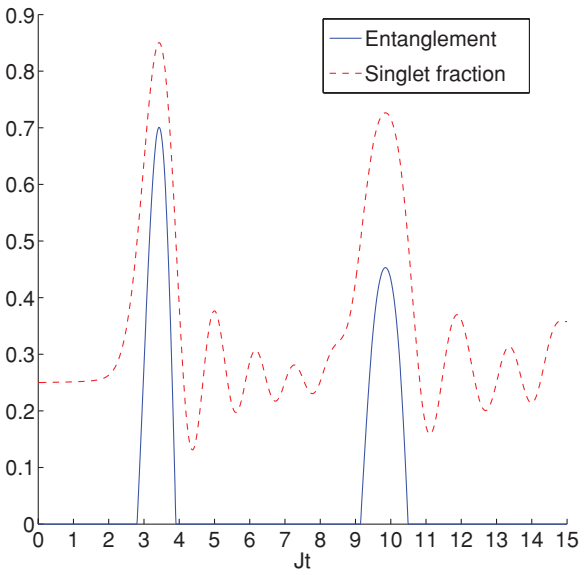

FIG. 1. (Color online) Entanglement and singlet fraction in terms of time for a chain of length $N = 20$ and $\Delta = 1$. Both axes in this figure and all other figures in this article are dimensionless.

entanglement, we plot the amount of entanglement in its first peak ($t = t_{\mathrm{opt}}$) in terms of anisotropy Δ for the chains with different lengths in Fig. 2(a) and the associated singlet fraction at the same time in Fig. 2(b). One interesting feature is that the entanglement transmitted dips on the XY side of $\Delta = -1$ and sharply rises on its FM side, which captures the first-order phase transition at this point. (That such a change in behavior is seen despite the finite size is interesting.) In addition, this transition is also marked by a steep rise in the time required to reach the first peak in entanglement. This is shown in the inset to Fig. 2(a), which also shows

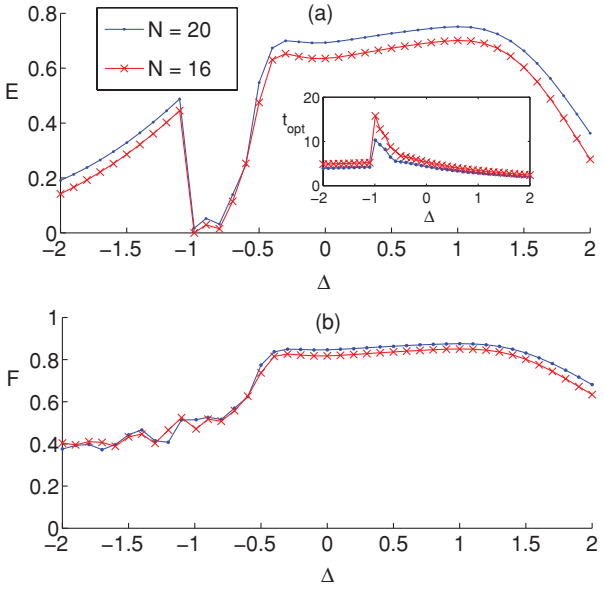

FIG. 2. (Color online) (a) Attainable entanglement in the first peak in terms of Δ for different lengths ($J = 1$). (Inset) The optimal time t_{opt} that the peak happens during the evolution. (b) Singlet fraction F at t_{opt} in a whole-phase diagram.

that the speed at which entanglement is propagated increases monotonically in the *XY* regime as one goes from $\Delta = -1$ to $\Delta = 1$. This fact is commensurate with the spin-wave velocity increasing with Δ as $\sin(\cos^{-1}\Delta)/\cos^{-1}\Delta$ in this regime [25], which we will discuss it in more detail later. In the *XY* phase we can recognize two distinct regimes. In its FM sector ($-1 < \Delta < 0$), entanglement falls rapidly by decreasing Δ, while in its AFM sector ($0 \leqslant \Delta \leqslant 1$), the entanglement is always good and increases by increasing Δ. After $\Delta = 1$, when the transition from the *XY* to the Néel phase happens, the entanglement starts falling with increasing Δ, as the Ising term $\sigma_j^z \sigma_{j+1}^z$ dominates, which by itself does not transfer entanglement. Note also a subtle feature that even outside the *XY* regime, for $\Delta > 1$, entanglement falls much slower with $|\Delta|$ than for $\Delta < -1$. In general, AFMs are thus better, even with similar degrees of anisotropy. Figure 2(a) also shows that the isotropic AFM Heisenberg interaction ($\Delta = 1$) not only is the best for transferring the highest amount of entanglement in the entire phase diagram, but also it has the highest speed in the *XY* phase. In Fig. 2(b), where singlet fraction F is plotted in the whole-phase diagram, in the FM phase ($\Delta < -1$) singlet fraction is always less than $1/2$, which shows that, despite the fact that entanglement is nonzero, quantum communication has no benefit over classical communication. The same thing will happen in the Néel phase when F becomes less than $1/2$ for quite large Δ's.

The effect of the length of the chain on the quality of transmission is shown in Fig. 3. We only concentrate on the best $\Delta = 1$ (isotropic AFM) point, as it is the best point in the phase diagram, and we compare the results with FM chains which have been predominantly studied so far. In Fig. 3(a) we plot the time at which the first peak in entanglement for different lengths. It is clear that the speed of entanglement transmission through the AFM ($J > 0$) chain is higher than that for the FM ($J < 0$) chain independent of the length. In Fig. 3(b) the amount of entanglement in the first peak is compared for both the AFM and the FM cases, from which it is clear that the entanglement transmitted in the case of the AFM chain has a distinctly higher value irrespective of length. Note also a visible even-odd effect on the amount of entanglement transmitted (and hence on two-time correlations), which will be interesting to observe in finite chains.

We have shown that in the absence of any of the sophisticated techniques for perfecting spin-chain communications, which come at a price and may be hard to implement, especially if one wanted to transfer information fast (i.e, refrain from very weak couplings), the isotropic AFM is the best channel in the entire phase diagram of the *XXZ* chain. We now estimate the efficiency with which local processing at the opposite ends of the spin chain and classical communication between them (a process called entanglement distillation [21]) can establish a *nearly perfect singlet* for an isotropic AFM channel. For instance, by using the recurrence algorithm for distillation [21] in a chain of length 10, for which entanglement $E = 0.8638$, starting from 9 impure pairs on average leads to a nearly singlet state with entanglement $E = 0.9920$ after seven iterations, and for a chain of length 20, for which entanglement $E = 0.7162$, we need to start with 17 impure pairs to get a singlet state with entanglement $E = 0.9926$ after nine iterations. This perfect singlet can then be used for sending quantum states perfectly through teleportation. It is worth pointing out that in different phases the spin chains represent different types of quantum channels. While in the FM phase, it is known to be an amplitude-damping channel (transmits $|0\rangle$ and $|1\rangle$ asymmetrically [2]), the $\Delta = 1$ point affects a so-called depolarizing channel (also noted in [13]), where $\rho_{0'N_{\rm ch}}$ is the mixture of the singlet state and the identity. Such $\rho_{0'N_{\rm ch}}$ is particularly suited for distillation protocols [21].

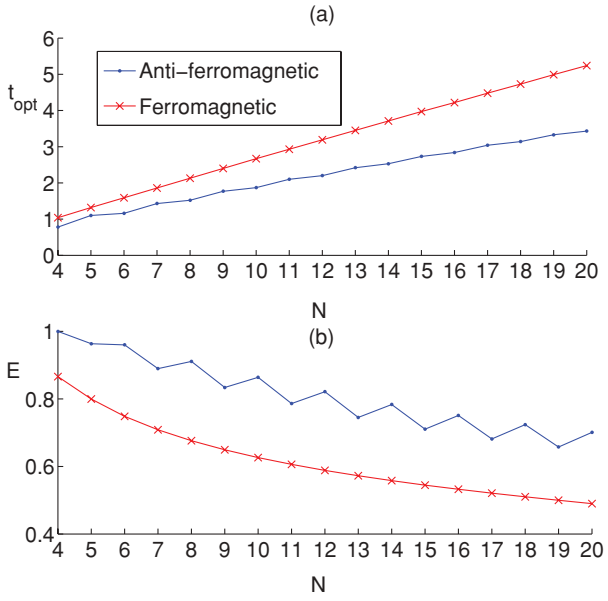

FIG. 3. (Color online) (a) Optimal time $t_{\rm opt}$ for both FM ($J = -1$) and AFM ($J = +1$) in terms of length N. (b) Entanglement at the first peak versus the length N for both FM ($J = -1$) and AFM ($J = +1$) chains when $\Delta = 1$.

V. EXPLANATION

When the phase of the system changes, not only does the Hamiltonian causing the time evolution vary, but the ground state, and consequently the initial state (9), also vary, and we have a different behavior for information transmission through the chain. The results in Fig. 2(a) show a dramatic and discontinuous change of entanglement at $\Delta = -1$ which is related to a first-order phase transition at this point and two completely different classes of ground states of the *XY* and the FM phases. At point $\Delta = +1$ entanglement falls continuously when we go from the *XY* phase to the Néel phase. This continuous change represents a second-order phase transition at this point. Beside these two phase transition points, there is a sharp drop of entanglement around $\Delta = -0.5$, which is very peculiar since there is no phase transition at this point. Also from the inset of Fig. 2(a) it is clear that the optimal time which one has to wait to get a peak goes up drastically for $\Delta < -0.5$. This strange property inside the *XY* phase is certainly not because of a phase transition. The reason for this slow dynamics and bad transmission is hidden behind an intrinsic property of the spin chain, namely, the spin-wave velocity.

Field theoretic techniques have been used to capture the asymptotic behavior of correlation functions in spin chains [26]. For the general *XXZ* Hamiltonian, it fails to get all

prefactors and exact solutions, but it is able to get the qualitative behavior of correlations successfully in the thermodynamic limit. Correlation functions in our problem are different from those obtained by field theory in at least two ways. First of all, we consider very finite chains, since the idea of using spin chains as quantum channels is valuable only for a finite distance. Second, all the dynamical correlations which are computed asymptotically are associated with the ground state of the system while in our problem correlations are computed for the initial state (9) which is *not* the ground state. Despite these differences, we still can use some well-known results of the field theoretic techniques. For example, the dynamical correlation functions in the XY phase ($-1 < \Delta < 1$) in the asymptotic thermodynamical limit have the following form [26]:

$$\left\langle \sigma_j^\alpha(0)\sigma_k^\alpha(t)\right\rangle \sim (-1)^{|j-k|}\frac{1}{\left(|j-k|^2 - v_F^2 t^2\right)^{1/2\eta_\alpha}}, \tag{15}$$

where $\alpha = x, y, z$ and

$$\eta_x = \eta_y = 1/\eta_z = 1 - \frac{\cos^{-1}\Delta}{\pi}. \tag{16}$$

Moreover, v_F in Eq. (15) is the spin-wave velocity (this quantifies the propagation velocity of excitations in the chain), which has the following form:

$$v_F \propto \frac{\sin(\cos^{-1}\Delta)}{\cos^{-1}\Delta}. \tag{17}$$

Unfortunately, the aforementioned asymptotic forms of $\langle\sigma_j^\alpha(0)\sigma_k^\alpha(t)\rangle$, valid for $|j-k| >> v_F t$, are *singular* specifically at $|j-k| \sim v_F t$, which is the regime relevant to optimal quantum communication from the jth to the kth site (i.e., when the information, possibly traveling at a velocity v_F, reaches its destination). So one can only use some aspects reliably from the previous formulas. One of these is the velocity v_F of propagation of the correlations (and hence information). In Fig. 4 we plot $1/v_F$ (which is for an infinite chain) and t_{opt} (for a chain of length $N = 20$) in terms of Δ. As Fig. 4 clearly shows, both of these quantities behave in a strikingly similar way (the gap between two curves is not important since one can multiply them by some constants). As a consequence, for $\Delta < -0.5$ the propagation velocity is very slow, and one has to wait a long time to receive some information at the other side of the chain. This very slow dynamics also means that we will get a sharp fall in the entanglement as well as all other quantities which propagate through the chain unless we are willing to wait for very, very long times.

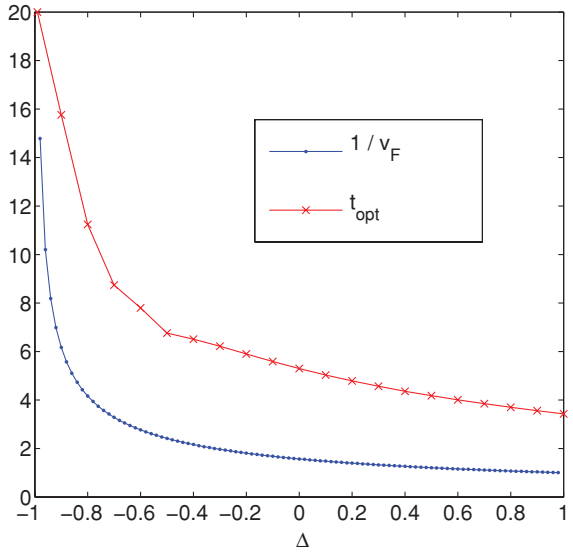

FIG. 4. (Color online) $1/v_F$ (for an infinite chain) and t_{opt} (for a chain of length $N = 20$) versus Δ.

As far as the question of why the isotropic ($\Delta = 1$ point) is the best point in the phase diagram in terms of a maximum of entanglement, recall that entanglement is given in terms of some dynamical correlation functions as in Eq. (13). Remember, though, that these correlations are *not* evaluated for the ground state and so cannot be strictly substituted by the known dynamical correlation functions to get any quantitative information, but perhaps only a qualitative picture, as we discuss. One can see from Eq. (15) that the $\Delta = 1$ point is the best for the propagation of correlations along the z direction. At points with $\Delta < 1$ the z component of correlations does not propagate as well as the x component, and, in fact, near to $\Delta = -1$ it is expected not to propagate at all ($\eta_z \approx \infty$). Thus, the term $-\frac{1}{2}\langle\sigma_0^z(0)\sigma_j^z(t)\rangle$ in Eq. (13) for entanglement, which is positive, contributes more and more as we approach $\Delta = 1$ and gives a higher entanglement. It is true that as we approach the isotropic point from $\Delta < 1$ side, the η_x rises (i.e., propagation of correlations in the x direction deteriorates somewhat). However, it must be that the gain from the better propagation of correlations in the z direction more than compensates for the deterioration of the propagation of correlations along the x direction. The reason is that η_z changes from ∞ to 1 (huge gain), while η_x only goes from 0 to 1.

As far as the intriguing dip after $\Delta = -0.5$ is concerned, we are not yet in a position to explain it. It seems that the behavior expected at $\Delta \to -1$, where both the velocity of correlations and their propagation quality along the z direction are worst, starts to happen quite a bit *before* the actual point.

VI. CHANNEL CHARACTERIZATION AND EVEN-ODD EFFECT

As is clear from Fig. 3(b), in the case of the AFM chain, entanglement has a zigzag behavior when N varies, while it behaves uniformly for FM chains. This even-odd effect for AFM chains has a fundamental reason. In even chains when $\Delta > -1$, the total magnetization of the ground state is always zero and because of the rotational symmetry in the ground state one can exchange all $|0\rangle$'s and $|1\rangle$'s while the ground state remains unchanged. In other words, in even chains for $\Delta > -1$ we always have

$$\sigma_x^{\otimes N_{\text{ch}}}|\psi_g\rangle_{\text{ch}} = |\psi_g\rangle_{\text{ch}}. \tag{18}$$

This symmetry, which is absent in FM chains and also in each of the doubly degenerate ground states of the odd chains, has a profound effect on the transmission characteristics of the chain. In even chains, the effect of the chain is completely recognized by the Kraus operators $\{\sqrt{p_I}I, \sqrt{p_x}\sigma_x, \sqrt{p_y}\sigma_y, \sqrt{p_z}\sigma_z\}$, where $p_{I,x,y,z}$ are positive and their summation is equal to 1, so one can explain the effect of this channel such that it applies

one of the Pauli operators (including identity) with some probability to the input state. Obviously, these probabilities are dependent on the length N, time t, and anisotropy Δ. So using the aforementioned Kraus operators we get the following form for the state $\rho_{0'N_{\rm ch}}$:

$$\rho_{0'N_{\rm ch}} = p_I(t)|\psi^-\rangle\langle\psi^-| + p_x(t)|\phi^-\rangle\langle\phi^-| + p_y(t)|\phi^+\rangle\langle\phi^+| + p_z(t)|\psi^+\rangle\langle\psi^+|, \quad (19)$$

where

$$|\psi^\pm\rangle = \frac{|01\rangle \pm |10\rangle}{\sqrt{2}}, \quad |\phi^\pm\rangle = \frac{|00\rangle \pm |11\rangle}{\sqrt{2}} \quad (20)$$

are Bell states. Thus, it means that $\rho_{0'N_{\rm ch}}$ is diagonalized in the Bell basis. This channel is called a *Pauli channel* in the literature. Since in the Hamiltonian (10) there is no difference between x and y directions, we always have $p_x = p_y$ for an XXZ chain. At the point $\Delta = 1$ where all directions become identical we have $p_x = p_y = p_z$ and the channel is the famous depolarizing channel.

For the case of odd N, characterization of the channel is not yet known and one can just consider it numerically. Since in odd chains the ground state of the system is degenerate, to take one of them we apply a small magnetic field in the z direction to break the symmetry. In this case, the total magnetization is ± 1 (dependent on the direction of the magnetic field: $\pm z$) and the symmetry (18) does not hold anymore.

For $\Delta < -1$, since the ground state is FM and all spins are aligned, the type of the channel is amplitude damping [2], so then the even-odd effect vanishes and the channel behaves uniformly for all N. It is worth mentioning that in entanglement distillation procedures [21], Werner states, which are a mixture of Bell states, are distilled more easily than the other states [21], so transferring the singlets through a Pauli channel has the advantage that the final state is very close to a Werner state (at $\Delta = 1$ it is exactly a Werner state) and one can distill them more easily than those which are gained through the transmission of other channels such as amplitude damping.

VII. THERMAL FLUCTUATIONS

Generally, when a system is in nonzero temperature, the state of the channel before evolution is described by a thermal state $\frac{e^{-\beta H_{\rm ch}}}{Z}$, instead of the ground state, where $\beta = 1/K_B T$ and Z is the partition function. So in this case the initial state of the system is

$$\rho(0) = |\psi^-\rangle\langle\psi^-| \otimes \frac{e^{-\beta H_{\rm ch}}}{Z}. \quad (21)$$

We assume that the thermalization time scale of the system is large so that one can consider the unitary dynamics starting the initial state (21). So, after time t the system evolves to $\rho(t) = U\rho(0)U^\dagger$ and the target state $\rho_{0'N_{\rm ch}}(t)$ can be gained as before by tracing out the bulk of the chain $\rho_{0'N_{\rm ch}}(t) = {\rm tr}_{0'\hat{N}_{\rm ch}}\{\rho(t)\}$. Entanglement of the state $\rho_{0'N_{\rm ch}}(t)$ at its optimal time is plotted in Fig. 5(a) in terms of initial temperature for both FM ($J = -1$) and AFM chains ($J = +1$). As is clear from the figure, increasing the temperature always destroys the entanglement but it has less effect on the AFM chain.

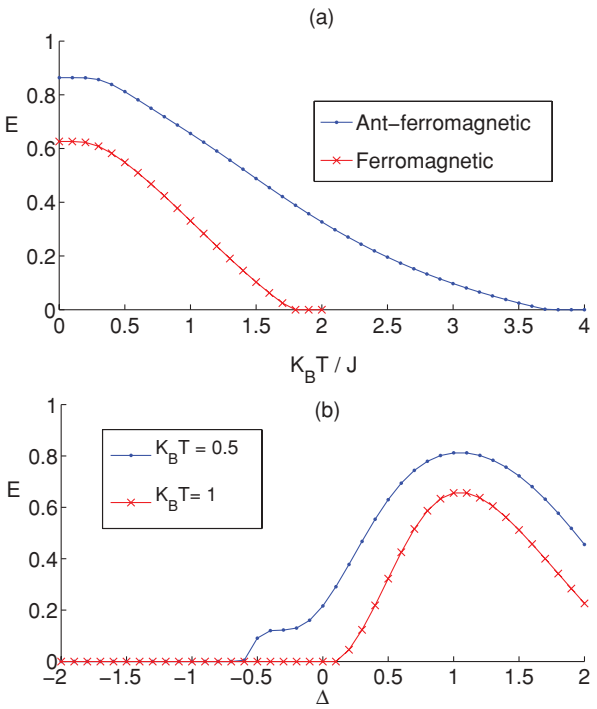

FIG. 5. (Color online) (a) Entanglement in terms of temperature in a chain of length $N = 10$ for the isotropic case ($\Delta = 1$) in both FM ($J = -1$) and AFM ($J = +1$) phase. (b) Entanglement in a whole-phase diagram for different temperatures in the chain of length $N = 10$.

In Fig. 5(b) the entanglement in the whole-phase diagram is plotted for different temperatures. When temperature rises, entanglement survives more for a fully symmetric Heisenberg point ($\Delta = 1$). Specially, the FM phase is highly sensitive to thermal fluctuations, and entanglement is destroyed rapidly when temperature rises. Furthermore, we found that the optimal time $t_{\rm opt}$ at which the entanglement peaks is almost independent of the temperature and varies very slowly in the whole-phase diagram.

VIII. INTERACTION WITH BATH AND DECOHERENCE EFFECT

In practical situations it is impossible to isolate a quantum system from its environment. In the case of Markovian interaction between the system and the environment, a Lindblad equation describes the evolution of the system

$$\dot{\rho} = -i[H, \rho] + \ell(\rho), \quad (22)$$

where $\ell(\rho)$ is the Markovian evolution of the state ρ. Let us assume an environment which has no preferred direction. Eventually, the interaction should have the form

$$\ell(\rho) = -\frac{\gamma}{3}\sum_i\sum_\alpha \{\rho - \sigma_i^\alpha \rho \sigma_i^\alpha\}, \quad (23)$$

where index i takes $0', 0, \ldots, N_{\rm ch}$, α gets x, y, z, and the coefficient γ stands for the rate of decoherence. In Fig. 6(a) we plot the entanglement in terms of noise strength γ for

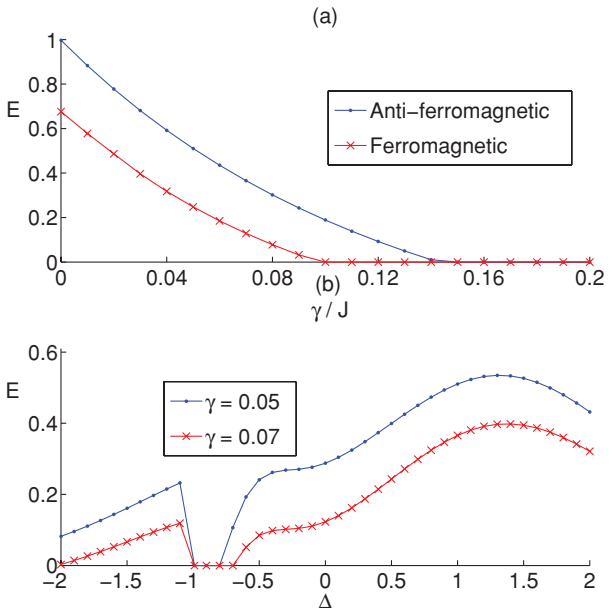

FIG. 6. (Color online) (a) Entanglement in terms γ in a chain of length $N = 8$ for the isotropic case ($\Delta = 1$) in both FM ($J = -1$) and AFM ($J = +1$) phase. (b) Entanglement in a whole-phase diagram for different noise strength γ in a chain of length $N = 8$.

both FM ($J = -1$) and AFM ($J = +1$) chains. The figure clearly shows that entanglement decays exponentially by increasing γ, but like the thermal effect the AFM chain is more resistive against Markovian noise. In Fig. 6(b), we plot the attained entanglement for when Δ varies in whole-phase diagram. As the figure shows, the noise effect always kills the entanglement and, similar to the thermal fluctuations, optimal time is almost independent of noise parameter γ. Surprisingly, the best point in the phase diagram is not the case of $\Delta = 1$ and it moves down inside the Néel phase. The reason for this interesting phenomena comes from the velocity of dynamics. Since the evolution in the Néel phase is faster [see the inset of Fig. 2(a)] and entanglement peaks earlier, decoherence has less opportunity to interfere and shows its destructive effect.

IX. CLASSICAL COMMUNICATION

We now comment on the classical information transmission through spin chains, which may be interesting for spintronics. To quantify the amount of classical information which each channel can transmit, the concept of the classical capacity has been introduced. The classical capacity of the channel ξ [introduced by the Kraus operators (1) in a very general case] gives the maximum amount of classical information that can be reliably transmitted per channel use. In calculating the classical capacity it is necessary to perform a maximization over multiple uses of the channel,

$$C = \max_n \frac{C_n}{n}, \tag{24}$$

where C_n is the classical capacity of the channel ξ which can be achieved if the sender is allowed to encode the information on codewords which are entangled only up to n-parallel channel uses. The value of C_n is obtained by maximizing the Holevo information [27] at the output of n parallel channel uses, over all possible input ensembles $\{p_i, \rho_i\}$; that is,

$$C_n = \max_{\{p_i,\rho_i\}} H_n(\xi^{\otimes n}, \{p_i, \rho_i\}), \tag{25}$$

where $H_n(\xi^{\otimes n}, \{p_i, \rho_i\})$ is the Holevo information which is defined as

$$H_n = \left\{ S\left[\xi^{\otimes n}\left(\sum_i p_i \rho_i\right)\right] - \sum_i p_i \xi^{\otimes n}(\rho_i)\right\}. \tag{26}$$

Here p_i's are probabilities, ρ_i's are n-qubit codewords (either entangled or separable) and S is the von Neumann entropy. Unfortunately, computing the classical capacity is an extremely hard task since it needs a very difficult maximization. However, recently the classical capacity of the depolarizing channel has been computed [28] and it was shown that this capacity can be achieved by encoding messages as products of pure states belonging to an orthogonal basis and using measurements which are products of projections onto this same orthogonal basis. So due to the fact that entanglement does not increase the capacity of the depolarizing channel, all maximization shrinks to compute the single-shot capacity C_1 as the real capacity of the channel.

As we discussed in Sec. IV, for even chains the *XXZ* Hamiltonian is a Pauli channel. At isotropic point ($\Delta = 1$) it is a depolarizing channel, for which C_1 is the real capacity and entangled inputs do not increase it. This motivates us to study *single-shot* classical capacity of the *XXZ* Hamiltonian for *pure orthogonal* input states. However, the single-shot capacity which is computed over pure orthogonal input states is not necessarily the real capacity of the channel (except at the point $\Delta = 1$) but at least it gives us a lower bound of the classical capacity. To have the form of a Pauli channel, we also restrict our study just to the even chains.

We start with the most general form of the orthogonal pure qubit states,

$$\begin{aligned} |\psi_1\rangle &= \cos\frac{\theta}{2}|0\rangle + e^{i\phi}\sin\frac{\theta}{2}|1\rangle \\ |\psi_2\rangle &= \sin\frac{\theta}{2}|0\rangle - e^{i\phi}\cos\frac{\theta}{2}|1\rangle, \end{aligned} \tag{27}$$

where $0 \leqslant \theta \leqslant \pi$ and $0 \leqslant \phi \leqslant 2\pi$. For the input ensemble, we associate the probability p_1 to the input state $\rho_1 = |\psi_1\rangle\langle\psi_1|$ and similarly probability p_2 to the state $\rho_2 = |\psi_2\rangle\langle\psi_2|$. When each of these states goes through the channel, we get

$$\begin{aligned} \xi(\rho_i) = p_I\rho_i + p_x\sigma_x\rho_i\sigma_x + p_y\sigma_y\rho_i\sigma_y + p_z\sigma_z\rho_i\sigma_z, \\ i = 1, 2, \end{aligned} \tag{28}$$

where $p_{I,x,y,z}$ are dependent on time t and anisotropy Δ. It is easy to see that $S(\xi(\rho_1))$ and $S(\xi(\rho_2))$ are equal and independent of ϕ. Thus, the second term in the Holevo information (26) is $p_1 S(\xi(\rho_1)) + p_2 S(\xi(\rho_2)) = S(\xi(\rho_1))$, which is independent of p_1 and p_2 and it is just dependent on θ. We can easily maximize the first term in the Holevo

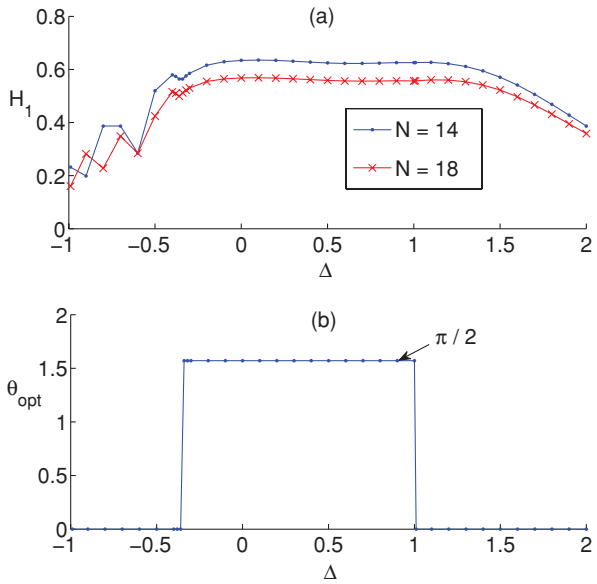

FIG. 7. (Color online) (a) Holevo information H_1 in terms of Δ for different lengths. (b) Optimal angle θ_{opt} for input set of states in terms of Δ.

information (26) for all values of θ by choosing $p_1 = p_2 = 1/2$ such that $S(\xi(p_1\rho_1 + p_2\rho_2)) = 1$, so to maximize the Holevo information H_1 one should just find $\theta = \theta_{\text{opt}}$ such that minimize $S(\xi(\rho_1))$.

Our analytic computation shows that

$$\theta_{\text{opt}} = \begin{cases} 0 \text{ or } \pi & \text{if } p_z > p_x, \\ \pi/2 & \text{if } p_z < p_x, \\ \text{arbitrary} & \text{if } p_z = p_x, \end{cases} \tag{29}$$

where the situation $p_z = p_x$ is associated to the depolarizing channel ($\Delta = 1$) which for any value of $0 \leqslant \theta \leqslant \pi$ the classical capacity is achieved. An important point is that the optimal input ensemble is independent of phase ϕ, which gives us a lot of degrees of freedom for input states. This also was expected due the symmetry of the x and the y directions in our Hamiltonian (10).

In Fig. 7(a), we plot the classical capacity in terms of Δ. This figure clearly shows that H_1 is quite flat in the XY phase and it suddenly falls for $\Delta < -0.5$. A more interesting result is shown in Fig. 7(b), where optimal θ is plotted in a whole-phase diagram. It shows that when we cross the point $\Delta = 1$ from the XY phase to the Néel phase, suddenly the optimal ensemble changes from orthogonal states on the equator ($\theta = \pi/2$) of the Bloch sphere to the states on the poles ($\theta = 0$). Within the XY phase, around $\Delta = -0.35$ the optimal input ensemble changes such that optimal states for $-1 < \Delta < -0.35$ are gained by $\theta = 0$ and for $-0.35 < \Delta < 1$ are obtained by $\theta = \pi/2$. In the the FM phase ($\Delta < -1$) the transmission is completely different and it is explained as an amplitude-damping channel [2]. For this channel it was shown that C_1 is achieved by the inputs given as Eq. (28) for $\theta = \pi/2$ [29].

It is interesting to check the classical capacity of the channel when it cannot transmit quantum information. So for a chain of length $N = 8$ with the noise parameter $\gamma = 0.3$, entanglement cannot be transferred because of the large noise (quantum information transmission is impossible), but at optimal times for isotropic case ($\Delta = 1$), one gains $C_1 = 0.3931$ for the AFM chain ($J = +1$) and $C_1 = 0.1453$ for the FM chain ($J = -1$).

X. ENTANGLEMENT PROPAGATION THROUGH THE CHAIN

A curious feature emerges in the propagation of entanglement through chains with even numbers of spins. For $\Delta \geqslant 0$, there is never any entanglement at any time between site $0'$ and odd sites, and entanglement seems to *hop* through the chain. If one takes an approach whereby one draws a solid line for the presence of strong entanglement and a dashed line for very weak entanglement (<0.1), the open-ended ground state will be *depicted* as a dimer (remember it is not an exact dimer) [30]. Appending a singlet of spins 0 and $0'$ at one end of the chain makes the total system look like a series of strongly entangled pairs next to each other (with weaker links between) and this is shown for the $N = 6$ case in Step 1 of Fig. 8(a). When the system evolves, the state of the system takes the form of Step 2 in Fig. 8(a) and after a while it goes to the form of Step 3 in Fig. 8(a). To explain this curious effect, without losing the generality, we consider the isotropic AFM. Clearly, the structure shown in Fig. 8(b), where a singlet between $0'$ and an odd site breaks three strong bonds, is energetically not favored in course of a unitary dynamics starting as Step 1 of Fig. 8(a). So, despite a finite (but small) overlap between the state shown in Fig. 8(b) and that in Fig. 8(a), this state does not emerge through the dynamics in the sense that its overlap with the state $|\psi(t)\rangle$ never becomes higher than a certain value. Quantitatively, all moments of Hamiltonian are conserved [12] during the evolution: $\forall n, \quad \langle H^n\rangle = \langle\psi(t)|H^n|\psi(t)\rangle = \langle\psi(0)|H^n|\psi(0)\rangle$, so energy ($E = \langle H\rangle$) and its variance ($\eta = \sqrt{\langle H^2\rangle - \langle H\rangle^2}$) are constant during the evolution. It means that only states with energy expectation $\bar{E}$ for which $E - \eta < \bar{E} < E + \eta$, such as in Fig. 8(a), can contribute in evolution, while those as in Fig. 8(b) cannot play a role. Note also that this curious phenomena, when recast in terms of two-time correlations, states that $\langle\sigma_0^z(0)\sigma_j^z(t)\rangle$ should be less than $-1/3$ only for the even sites j. Thus, in potential physical systems where such

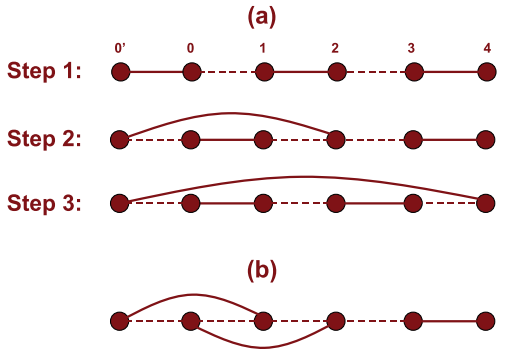

FIG. 8. (Color online) (a) Entanglement between site $0'$ and other sites in the chain during the evolution in an AFM chain ($\Delta = 1$) of length $N = 6$. (b) One configuration of the states which are not accessible energetically.

dynamical correlations is measurable, the hopping mode of transfer should be testable.

XI. POTENTIAL PHYSICAL REALIZATIONS

We now mention some systems in which our results can be potentially tested, though there is some way to go for some of these systems, as local addressing of the spin to be suddenly coupled to the chain may be required. Recently, there has been extensive interest in finite spin chains such as fabricated AFM nanochains [15], and especially even-odd effects in such systems [31]. This can be one potential system where recently developed sensitive magnetometers [32] can perhaps be used for verifying the correlations and hence entanglement. Perhaps an STM tip encoding the spin to be transmitted can be brought close to one end of a finite array. Finite chains of doped fullerines in nanotubes [33] (such as AFM $Sc@C_{82}$ [16]) is the other alternative for developing this idea. Spins in such systems have already been measured, and perhaps local electrical gates can give local control to couple in the input qubit [33]. Optical superlattices with atoms can realize an ensemble of finite spin chains [34], as well as the switching on their interactions [35]. Barrier heights at regular intervals may be raised to create arrays of small lattice segments (cells) of sizes 2 and $N_{\rm ch}$ with the repeating pattern $2, N_{\rm ch}, 2, N_{\rm ch}, \ldots$. The $0'0$ singlet and the finite chain ground states can be created in the cells of sizes 2 and $N_{\rm ch}$, respectively, as ground states (in fact, the former has already been accomplished [34]). Next, again through global methods, the barriers between the 2 site cells and the $N_{\rm ch}$ site cells to their right have to be lowered (simultaneously the barrier between the two sites of the cell of length 2 has to be raised) so as to form superlattices with cells of size $N_{\rm ch}+2$ each. The subsequent dynamics will then be exactly as we have predicted and can potentially be verified through global time-of-flight correlation measurements [34]. One can use ion traps where small spin systems are being realized [36], as well as implementing spin chains with trapped electrons [37] where initializing individual spins and controlling the interaction at one end are both simple. NMR is another fruitful avenue for testing communication through spin chains [38].

XII. SUMMARY

We have studied the transmission of both classical and quantum information through the all phases of the *XXZ* Hamiltonian. This quantifies the ability of each phase for information transmission through its natural dynamics. We found that in the absence of noise and thermal fluctuation isotropic Heisenberg Hamiltonian ($\Delta = 1$) is the best point of the phase diagram for information transmission, in terms of both its amount and its speed. This is indeed important since the natural interaction of many spin-chain realizations is the fully symmetric Heisenberg interaction. The speed of propagation of the information, despite our finite open-ended case, fits strikingly well with the spin-wave velocities known from continuum limit field theoretic studies of the *XXZ* spin chain. When decoherence and thermal fluctuations are taken to account, the best point of the phase diagram moves to the Néel phase, which due to a faster evolution, is less sensitive to these sources of noise. This clearly shows why faster dynamics are more encouraging to minimize the destruction effects such as the thermal fluctuations and decoherence. Furthermore, we showed that the transmission through an even chain is characterized by the Pauli channel, which has benefits in terms of immediate applicability of entanglement distillation. We also studied the transmission of classical information through this channel. Optimal states for single-shot classical capacity were identified and we realized that even when system is so noisy, such that quantum information is completely destroyed, some classical information can be transferred. Studying the entanglement propagation through the chain showed that entanglement skips odd-numbered sites and manifests as a curious behavior of two-time correlation functions during the nonequilibrium dynamics. It remains an open problem to explain well the mysterious behavior of the dynamics which entanglement suddenly drops around the point $\Delta = -0.5$.

ACKNOWLEDGMENTS

S.B. received support from EPSRC, through which A.B. is funded. S.B. is also supported by the QIP IRC, the Royal Society, and the Wolfson Foundation.

[1] L. Amico *et al.*, Rev. Mod. Phys. **80**, 517 (2008).
[2] S. Bose, Phys. Rev. Lett. **91**, 207901 (2003).
[3] S. Bose, Contemp. Phys. **48**, 13 (2007).
[4] M. Christandl, N. Datta, A. Ekert, and A. J. Landahl, Phys. Rev. Lett. **92**, 187902 (2004); M. B. Plenio and F. L. Semiao, New J. Phys. **7**, 73 (2005); A. Wojcik, T. Luczak, P. Kurzynski, A. Grudka, T. Gdala, and M. Bednarska, Phys. Rev. A **72**, 034303 (2005); A. Kay, Phys. Rev. Lett. **98**, 010501 (2007); C. Di Franco, M. Paternostro, and M. S. Kim, Phys. Rev. Lett. **101**, 230502 (2008).
[5] T. J. Osborne and N. Linden, Phys. Rev. A **69**, 052315 (2004); D. Burgarth and S. Bose, *ibid.* **71**, 052315 (2005).
[6] J. Fitzsimons and J. Twamley, Phys. Rev. Lett. **97**, 090502 (2006).
[7] A. Bayat and V. Karimipour, Phys. Rev. A **71**, 042330 (2005).
[8] D. Burgarth and S. Bose, Phys. Rev. A **73**, 062321 (2006).
[9] V. Giovannetti and D. Burgarth, Phys. Rev. Lett. **96**, 030501 (2006).
[10] A. Bayat and S. Bose, e-print arXiv:0706.4176 (to appear in Advances in Mathematical Physics).
[11] O. Romero-Isart, K. Eckert, and A. Sanpera, Phys. Rev. A **75**, 050303(R) (2007).
[12] M. J. Hartmann, M. E. Reuter, and M. B. Plenio, New J. Phys. **8**, 94 (2006).
[13] L. Campos Venuti, C. Degli Esposti Boschi, and M. Roncaglia, Phys. Rev. Lett. **99**, 060401 (2007).
[14] H. Mikeska and A. Kolezhuk, Lect. Notes Phys. **645**, 1 (2004).
[15] C. F. Hirjibehedin *et al.*, Science **312**, 1021 (2006).
[16] Yasuhiro Ito *et al.*, Chem. Phys. Chem. **8**, 1019 (2007).

[17] A. Flesch, M. Cramer, I. P. McCulloch, U. Schollwock, and J. Eisert, Phys. Rev. A **78**, 033608 (2008).
[18] C. H. Bennett, G. Brassard, C. Crepeau, R. Jozsa, A. Peres, and W. K. Wootters, Phys. Rev. Lett. **70**, 1895 (1993).
[19] M. Horodecki, P. Horodecki, and R. Horodecki, Phys. Rev. A **60**, 1888 (1999).
[20] G. Bowen and S. Bose, Phys. Rev. Lett. **87**, 267901 (2001).
[21] C. H. Bennett, D. P. DiVincenzo, J. A. Smolin, and W. K. Wootters, Phys. Rev. A **54**, 3824 (1996).
[22] H. Wichterich and S. Bose, Phys. Rev. A **79**, 060302(R) (2009); P. Sodano, A. Bayat, and S. Bose, e-print arXiv:0811.2677.
[23] X. Wang and P. Zanardi, Phys. Lett. A **301**, 1 (2002).
[24] W. K. Wootters, Phys. Rev. Lett. **80**, 2245 (1998).
[25] O. S. Sariyer, A. N. Berker, and M. Hinczewski, Phys. Rev. B **77**, 134413 (2008).
[26] K. Fabricius, U. Low, and J. Stolze, Phys. Rev. B **55**, 5833 (1997).
[27] A. S. Holevo, IEEE Trans. Inform. Theory **44**, 269 (1998).
[28] C. King, IEEE Trans. Inf. Theory **49**, 221 (2003).
[29] V. Giovannetti and R. Fazio, Phys. Rev. A **71**, 032314 (2005).
[30] T. Wang, X. Wang, and Z. Sun, Physica A **383**, 316 (2007).
[31] S. Lounis, Ph. Mavropoulos, P. H. Dederichs, and S. Blugel, Phys. Rev. B **72**, 224437 (2005).
[32] J. M. Taylor *et al.*, Nat. Phys. **4**, 810 (2008).
[33] S. C. Benjamin *et al.*, J. Phys. Condens. Matter **18**, S867 (2006).
[34] S. Folling *et al.*, Nature (London) **448**, 1029 (2007).
[35] L.-M. Duan, E. Demler, and M. D. Lukin, Phys. Rev. Lett. **91**, 090402 (2003).
[36] A. Friedenauer *et al.*, Nat. Phys. **4**, 757 (2008).
[37] G. Ciaramicoli, I. Marzoli, and P. Tombesi, Phys. Rev. A **75**, 032348 (2007).
[38] J. Fitzsimons, L. Xiao, S. C. Benjamin, and J. A. Jones, Phys. Rev. Lett. **99**, 030501 (2007); J. Zhang, N. Rajendran, X. Peng, and D. Suter, Phys. Rev. A **76**, 012317 (2007); P. Cappellaro, C. Ramanathan, and D. G. Cory, Phys. Rev. Lett. **99**, 250506 (2007).